

THE EXPERIMENTAL IDENTIFICATION OF INDIVIDUAL PARTICLES BY THE OBSERVATION OF TRANSITION RADIATION IN THE X-RAY REGION

F HARRIS, T KATSURA, S PARKER and V Z PETERSON

Department of Physics, University of Hawaii, Hawaii, U S A

R W ELLSWORTH and G B YODH

Department of Physics, University of Maryland, Maryland, U S A

W W M ALLISON, C B BROOKS, J H COBB and J H MULVEY

Nuclear Physics Laboratory, Oxford University, Oxford, England

Received 13 November 1972

Transition radiation in the X-ray region produced by 1.3 GeV/c and 3.0 GeV/c electrons has been detected using multi-wire proportional chambers (MWPC). The radiation was generated in eleven stacks of 100 mylar foils (thickness $\frac{1}{2}$ mil or $\frac{1}{8}$ mil) each preceding one of eleven MWPC placed in line, two inch thick slabs of styrofoam were also used. The incident particles,

electrons or π^- -mesons, passed through the MWPC as well as the foils. Results are given on the numbers of transition radiation photons detected, the energy deposition in the chambers and the relativistic rise of ionisation loss in argon and krypton. The distribution in total pulse height obtained with krypton shows a good separation of π^- -mesons and electrons at 3 GeV/c.

1. Introduction

The phenomenon of transition radiation, first predicted by Ginzberg and Frank¹⁾ has been explored extensively by groups in the USSR²⁻⁵⁾ and also by Yuan and his collaborators at Brookhaven⁶⁻⁹⁾. Our intention in the experiment to be described in this report was to study the possibility of using this effect to identify efficiently individual particles of very high γ (i.e. $\gamma = E/m > 1000$). The results¹⁰⁾ confirm the predictions of others^{2,4,9,11)} that individual particles can be identified. The experiment was conducted at the Bevatron in December 1971 using two sets of foil radiators and one set of styrofoam radiators (see section 2.2). We defer comparison with theoretical predictions of transition radiation yield to a later report, following a more comprehensive series of experiments which have been performed at SLAC this summer. A good review of the theoretical basis is given by Garibian⁵⁾.

2. The experiment

2.1. METHOD

The method is to detect the X-rays emitted when a charged particle traverses an interface separating two media of different refractive index, in this case mylar-air. Since the probability of emission is $\sim \alpha$ per interface the effect must be amplified by the use of many

interfaces, such as a series of mylar foils. This is made possible by the fact that the X-rays are highly collimated along the particle trajectory, the typical emission angle being $\sim 1/\gamma$.

However, absorption of the X-rays in the foils limits the number of foils that can be effective. In addition, interference between the radiation emitted at the two foil surfaces results in a yield which decreases proportionally to t^2 when t (the foil thickness) falls below t_f the "formation zone"⁵⁾ for the foil material¹²⁾.

The compromise between primary yield and absorption leads to an arrangement in which a series of radiators (each consisting of about 100 foils) are interleaved with X-ray detectors (see fig. 1). A multiwire proportional chamber (MWPC) is an excellent detector of transition-radiation, especially if filled with a high Z gas such as krypton or xenon: the efficiency is good for X-rays in the 3-20 keV region, the ionization loss by the charged particle is low, the angular acceptance is high and if necessary several contemporaneous particles can be spatially resolved and so separately identified (by virtue of the $1/\gamma$ emission angle the transition radiation photons remain close to the parent particle trajectory).

2.2. APPARATUS

In this experiment we used 11 MWPC each preceded by radiator stacks containing 100 mylar foils. Two

radiator configurations were used foil thickness, $t = \frac{1}{6}$ mil¹³⁾ and air-spacing, $d = 60$ mil, $t = \frac{1}{2}$ mil with $d = 30$ mil

The chambers had a sensitive volume of $20 \text{ cm} \times 20 \text{ cm} \times 1.5 \text{ cm}$ and their construction has been described by Parker et al¹⁴⁾ For this experiment all the signal-wires were strapped together and one pulse height recorded for each chamber. Two gas fillings were used 93% argon + 7% methane and 93% krypton¹⁵⁾ + 7% methane. The chamber windows were $\frac{1}{4}$ mil aluminized mylar.

Data were taken at two values of beam momentum 1.3 GeV/c and 3 GeV/c. The experimental layout is shown in fig 1. In addition to three beam defining scintillation counters, three Cherenkov counters and a lead-lucite shower counter were used to identify the small percentage of electrons in the negatively charged beam ($\approx 0.2\%$ at 3 GeV/c and $\approx 2.2\%$ at 1.3 GeV/c). The π^- -meson contamination of 3 GeV electron triggers was measured to be much less than 1%.

The effect of bremsstrahlung and δ -rays produced in the foils was estimated to be negligible. However, to determine background from such processes runs were made in which the radiators were replaced with single sheets of plastic of the same total thickness and also others with no material present.

The charge from each chamber was readout with a

preamplifier and sample-and-hold. All eleven chamber signals and the shower counter pulse height were displayed on a CRT to be recorded on 35 mm film. In addition the signal from chamber 1, delayed by 200 ns, was taken direct to the CRT and also displayed so that in the analysis stage all events in which another particle had traversed the system within the integration time of the sample-and-hold ($\approx 3 \mu\text{s}$) could be excluded. On average $\approx 12\%$ of recorded events were rejected for this reason, the time distribution of double pulses indicates that in the worst case less than 4% of the remaining events were unresolved two particle events.

All the data recorded on film was measured by the Oxford PEPR¹⁶⁾, about 80 000 frames in 36 h.

2.3 ENERGY CALIBRATION

At frequent intervals during the runs each chamber was exposed to an ^{55}Fe X-ray source (5.9 keV) and calibration data recorded, also on film.

These measurements showed a systematic variation of the chamber gains with time; all chambers followed the same pattern which had a full excursion of $\approx 20\%$ over the 24 h in which most of the data was taken. This effect was probably due to pressure and temperature changes. The ^{55}Fe data were used to correct for this chamber-independent variation.

In the normal (data taking) mode of readout the

NOT TO SCALE

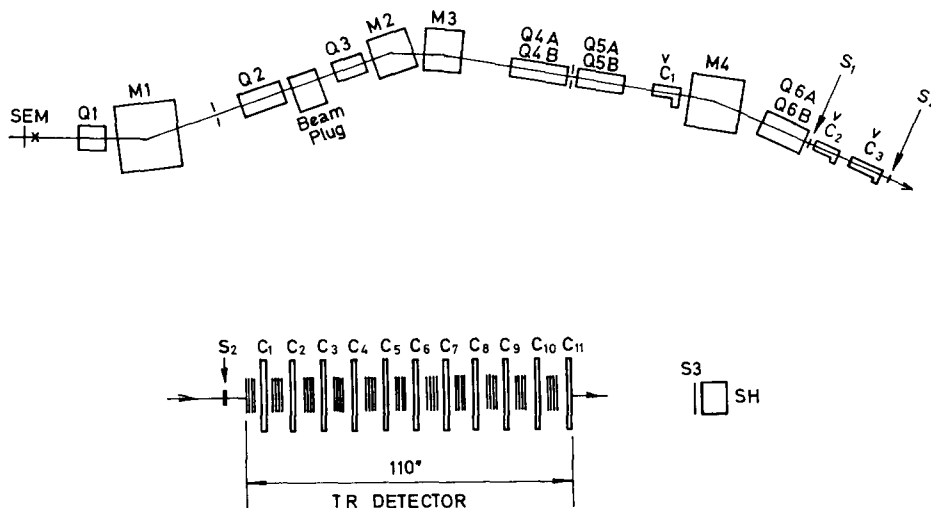


Fig 1 Diagram of beam and transition radiation detector

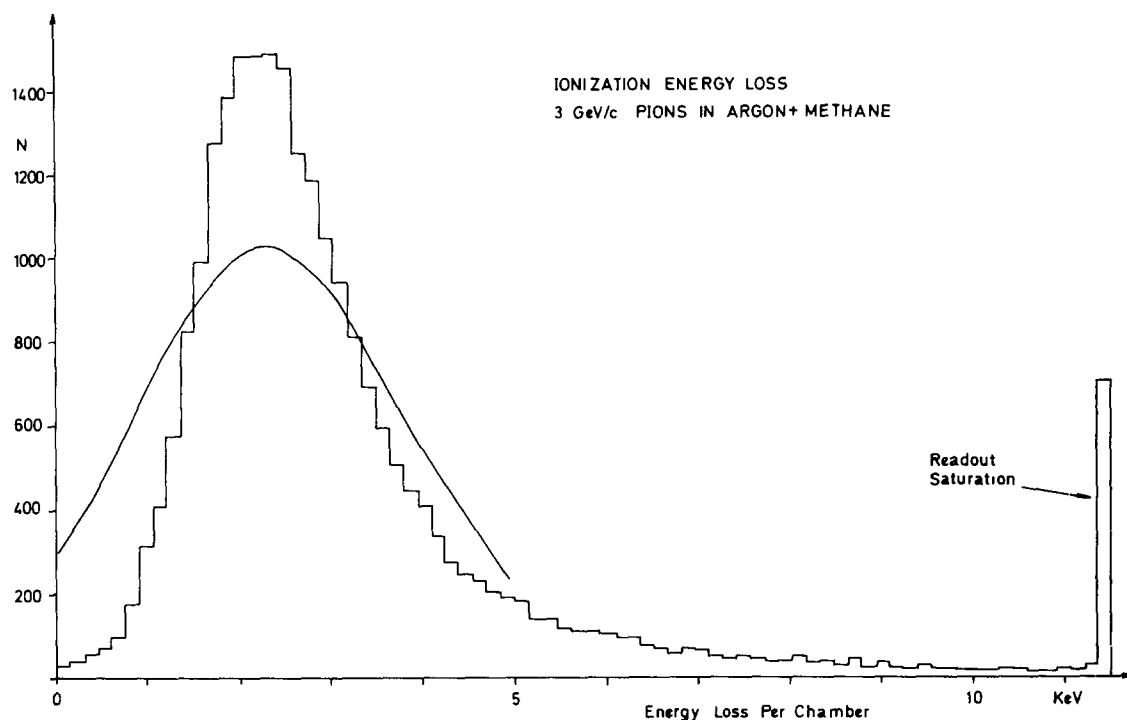


Fig 2a Distribution of ionization energy loss in a single chamber for 3 GeV/c π^- -mesons. The curve shows the predictions of Blunck and Leisegang¹⁷⁾. The chamber thickness is 2.5×10^{-3} g cm⁻² and the gas 93% argon and 7% methane.

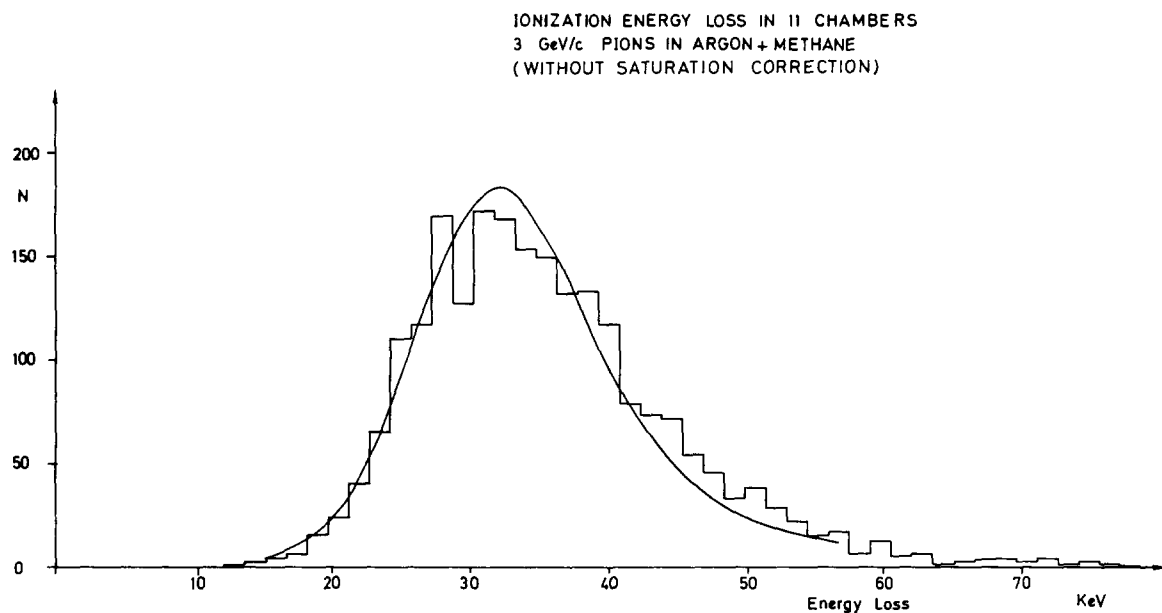


Fig 2b Distribution of ionization energy loss for 3 GeV/c π^- -mesons when signals from eleven chambers are added. The curve is the Blunck and Leisegang prediction treating the system as one chamber of thickness 27.3×10^{-3} g cm⁻² containing 93% argon and 7% methane.

trigger was provided by the beam particle selection logic, the ^{55}Fe X-rays on the other hand had to be self-triggered. When measurements were made taking

the output of a single chamber preamplifier directly to a pulse-height-analyser, a different relative pulse-height from ^{55}Fe X-rays and the peak of the $3\text{ GeV}/c\ \pi^-$

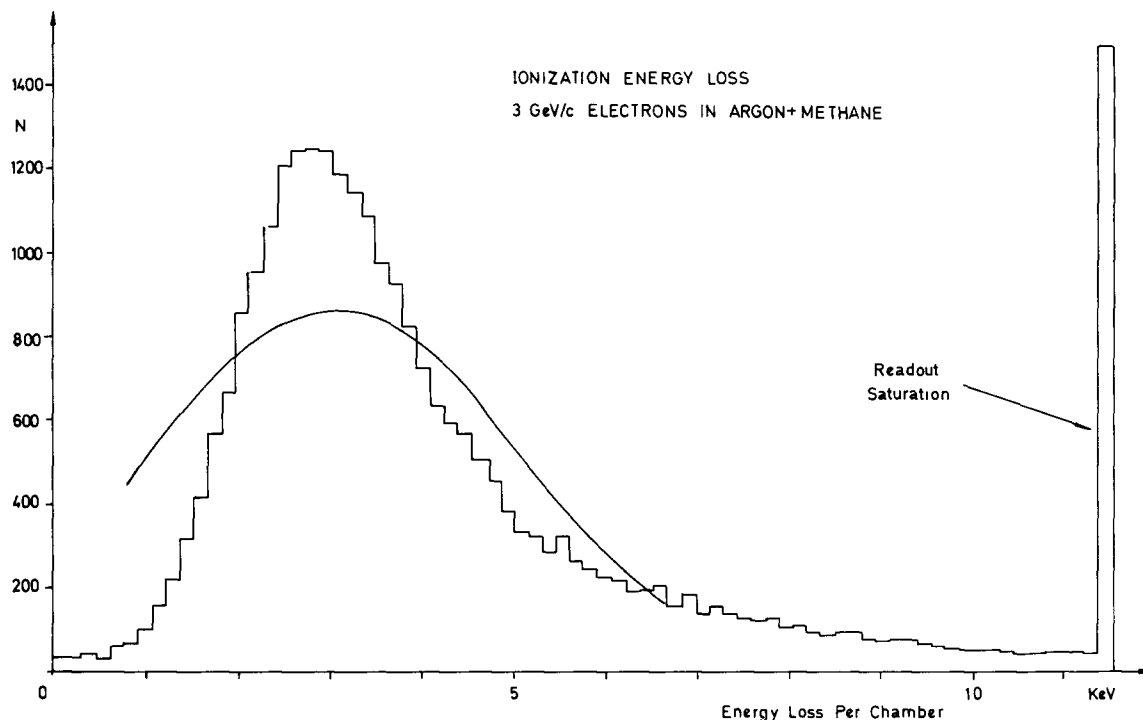


Fig 3a Distribution of ionization energy loss for 3 GeV/c electrons in single chamber containing 93% argon and 7% methane. The curve is the Blunck and Leisegang prediction.

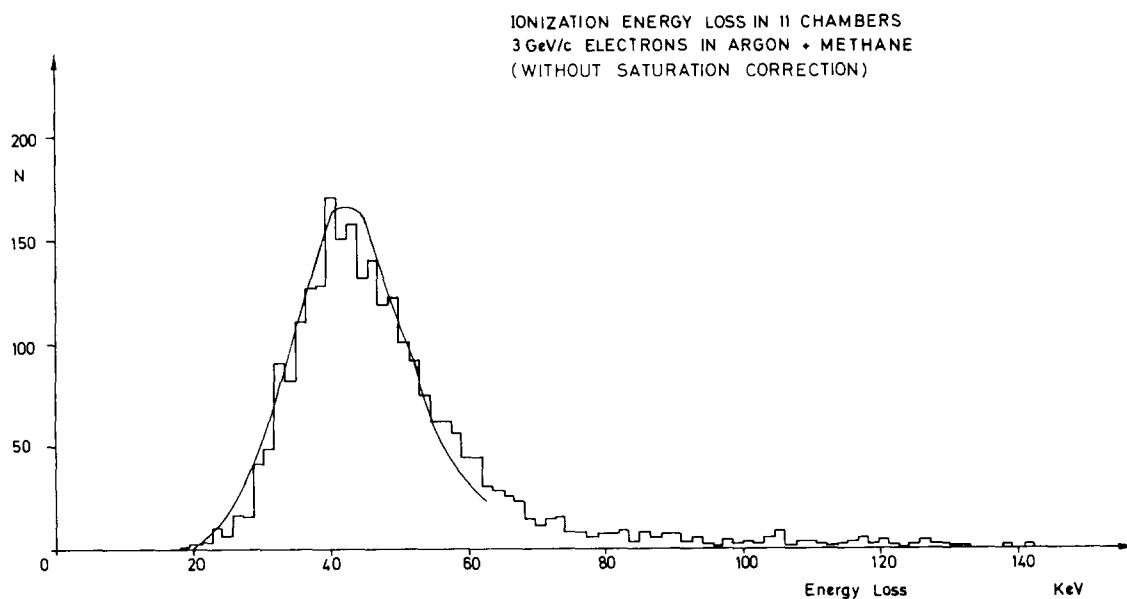


Fig 3b Distribution of sum of eleven chambers for ionization loss by 3 GeV/c electrons. The curve is the Blunck and Leisegang prediction treating the system as one chamber of thickness $27.3 \times 10^{-3} \text{ g cm}^{-2}$ containing 93% argon and 7% methane.

ionization loss distribution was obtained. We attribute the difference observed between the two modes to a systematic loss suffered by the signal from ^{55}Fe X-rays in the self-triggered normal readout due to delays in the trigger circuit. Consequently we have chosen the ^{55}Fe and $3\text{ GeV}/c\ \pi^-$ data taken with the direct readout to a pulse height analyser as the basis of our absolute energy calibration, however we must assign an uncertainty of at most 20% to this calibration procedure.

Although the linearity of chamber response was established beyond the range of interest the readout system (including CRT display) introduced a saturation effect which was not the same in magnitude for all chambers. The saturation level varied between 11.5 keV and 21 keV, in figures showing distributions of chamber pulse height all data above the lowest saturation level are shown in one overflow bin.

3. Results

3.1 THE DISTRIBUTION OF IONIZATION LOSS AND THE RELATIVISTIC RISE

We show in fig 2a the distribution of ionization loss by $3\text{ GeV}/c\ \pi^-$ -mesons in a single argon + methane filled chamber (data taken without radiators),

fig 2b shows the distribution obtained when the signals from 11 chambers are summed. The curves are the predictions of Blunck and Leisegang¹⁷⁾. As observed by others¹⁸⁻²⁰⁾ the experimental distribution is narrower than the Blunck-Leisegang theory for the single chamber, but agreement is reasonable for the "sum of 11" if the system is treated as a single chamber of thickness $11 \times 1.5\text{ cm}^2$ ²¹⁾. Figs 3a and 3b show the same distributions for $3\text{ GeV}/c$ electrons. Our widths (fwhm) agree well with the data of West²²⁾.

The data show the presence of the relativistic rise. Fig 4 shows our measurements of the relative most-probable energy loss, for both π^- -mesons and electrons, in a single chamber filled with argon + methane and also krypton + methane. The curves are predictions from Sternheimer and Peierls²³⁾ and the data are normalised to them at the $3\text{ GeV}/c\ \pi^-$ points (there is no density-effect correction for π^- -meson momenta below $\approx 14\text{ GeV}/c$). For $3\text{ GeV}/c\ \pi^-$ -mesons ($\gamma = 21.6$) the Sternheimer and Peierls prediction of most-probable energy loss per chamber with argon + methane filling is 2.3 keV compared with our measured value of $(2.2 \pm 0.1)\text{ keV}$, the corresponding figures for krypton + methane are 4.3 keV and $(4.2 \pm 0.2)\text{ keV}$. But these values are subject to an uncertainty in energy calibration of up to 20% (see section 2.3).

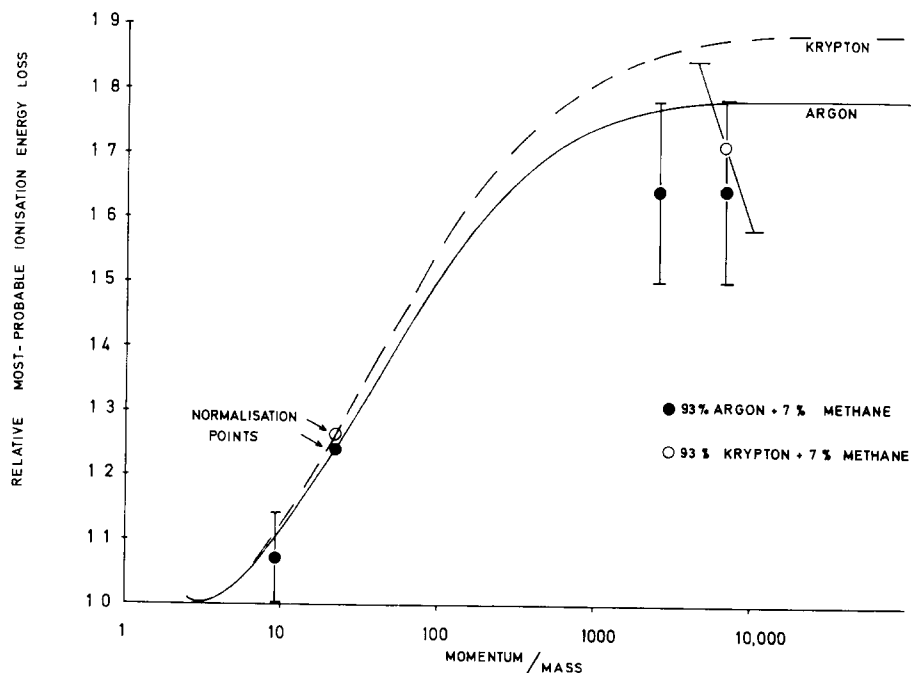


Fig 4 Relative most-probable energy loss as a function of the ratio momentum/mass. Points marked ● are for 93% argon + 7% methane, and those marked ○ are for 93% krypton + 7% methane. The curves have been calculated from Sternheimer and Peierls²³⁾. The relative ionization has been normalised to the calculated values at the points corresponding to the $3\text{ GeV}/c\ \pi^-$ -meson data (there is no density correction for π^- -meson momenta below $\approx 14\text{ GeV}/c$).

TABLE I
Ionization energy loss

Chamber gas	Momentum and particle	γ	Measured most-probable energy loss per chamber (subject to $\approx 20\%$ calibration uncertainty) (keV) ^a	Full-width-half-maximum (keV) ^a	Relative most-probable ionization energy loss per chamber normalised to Sternheimer-Peierls ²³ for 3 GeV/c π -meson	
					Experiment	Prediction
Argon	1.3 GeV/c π^-	9.4	1.9 ± 0.1	2.0	1.07 ± 0.07	1.11
	3.0 GeV/c π^-	21.6	2.2 ± 0.1	2.1	1.24	1.24
	1.3 GeV/c e^-	2.550	2.9 ± 0.2	2.6	1.64 ± 0.14	1.77
	3.0 GeV/c e^-	5.880	2.9 ± 0.2	2.4	1.64 ± 0.14	1.78
Krypton	3.0 GeV/c π^-	21.6	4.2 ± 0.2	3.3	1.26	1.26
	3.0 GeV/c e^-	5.880	5.7 ± 0.3	4.5	1.71 ± 0.13	1.87

See section 2.3, the overall 20% uncertainty in energy calibration is not included in the errors given

Other data are given in table 1, in agreement with other experiments²⁰) these results suggest that the plateau reached by the ionization loss at large γ is not as high as is predicted by Sternheimer and Peierls

3.2. TRANSITION RADIATION

When 3 GeV/c electrons pass through the system

with the $\frac{1}{2}$ mil mylar radiators in place the single chamber pulse-height distribution obtained is the histogram shown in fig 5a. By comparison with fig 3a, obtained without radiators (actually equivalent absorber and no absorber data combined), it is clear that there is an additional source of energy deposition; this we ascribe to transition radiation

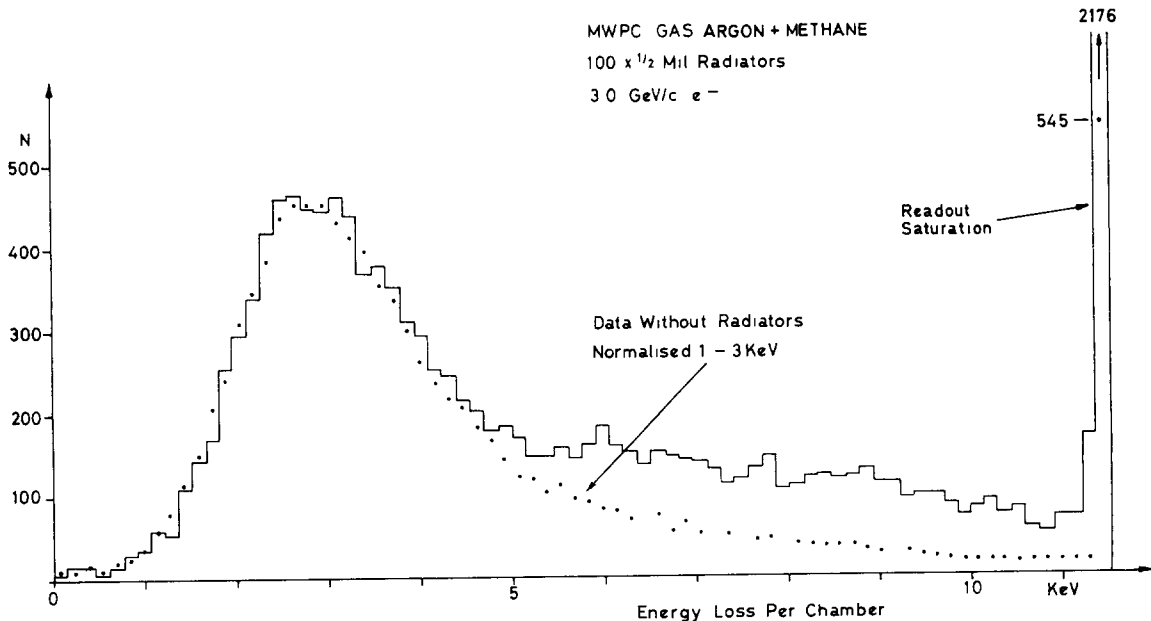


Fig 5a Distribution of energy deposited in a single argon/methane filled chamber when 3 GeV/c electrons pass through the $\frac{1}{2}$ mil mylar radiators. The points marked with a dot show the distribution obtained *without* radiators when this is normalized to have equal area in the 1 keV to 3 keV region

TABLE 2
Transition radiation

	Momentum and particle	Gas	Radiator	γ	11 chamber totals/incident particle (keV) ^a		
					Lower limit no of detected photons	Lower limit total energy deposition	Ionization loss energy deposition
1	3.0 GeV/c π	Argon	100, $\frac{1}{2}$ mil	21.6	0.3 ± 1	36.5 ± 1.8	35.2 ± 1.8
2	1.3 GeV/c e^-		100, $\frac{1}{2}$ mil	2.550	2.5 ± 0.8	57.5 ± 2.8	45.0 ± 2.2
3	3.0 GeV/c e^-		100, $\frac{1}{2}$ mil	5.880	3.6 ± 0.7	70.0 ± 3.5	48.6 ± 2.4
4	1.3 GeV/c e^-		100, $\frac{1}{2}$ mil	2.550	1.0 ± 1.0	51.6 ± 2.5	45.0 ± 2.2
5	3.0 GeV/c e^-		100, $\frac{1}{2}$ mil	5.880	2.0 ± 0.8	56.6 ± 2.8	48.6 ± 2.4
6	3.0 GeV/c e^-		1.50 mil	5.880	0.3 ± 1	48.5 ± 2.4	47.0 ± 2.3
7	3.0 GeV/c e^-		100, $\frac{1}{2}$ mil (tilted 30°)	5.880	3.3 ± 0.7	67.6 ± 3.3	48.6 ± 2.4
8	3.0 GeV/c e^-	Krypton	2" styrofoam	5.880	1.4 ± 1	57.5 ± 2.8	48.6 ± 2.4
9	3.0 GeV/c e^-		100, $\frac{1}{2}$ mil	5.880	5.0 ± 0.5	122 ± 6.1	85.6 ± 4.2
10	3.0 GeV/c e^-		100, $\frac{1}{2}$ mil	5.880	2.6 ± 0.7	100 ± 5.0	85.6 ± 4.2

^a See section 2.3, there is an overall 20% uncertainty in energy calibration which is not included in the errors given

The with and without-radiator distributions can be compared quantitatively in the following way. Self-absorption in the foils effectively removes all photons

of less than 3 keV, also in argon there are few examples of ionization loss less than 1 keV per chamber, therefore almost none of the pulses less than 4 keV should

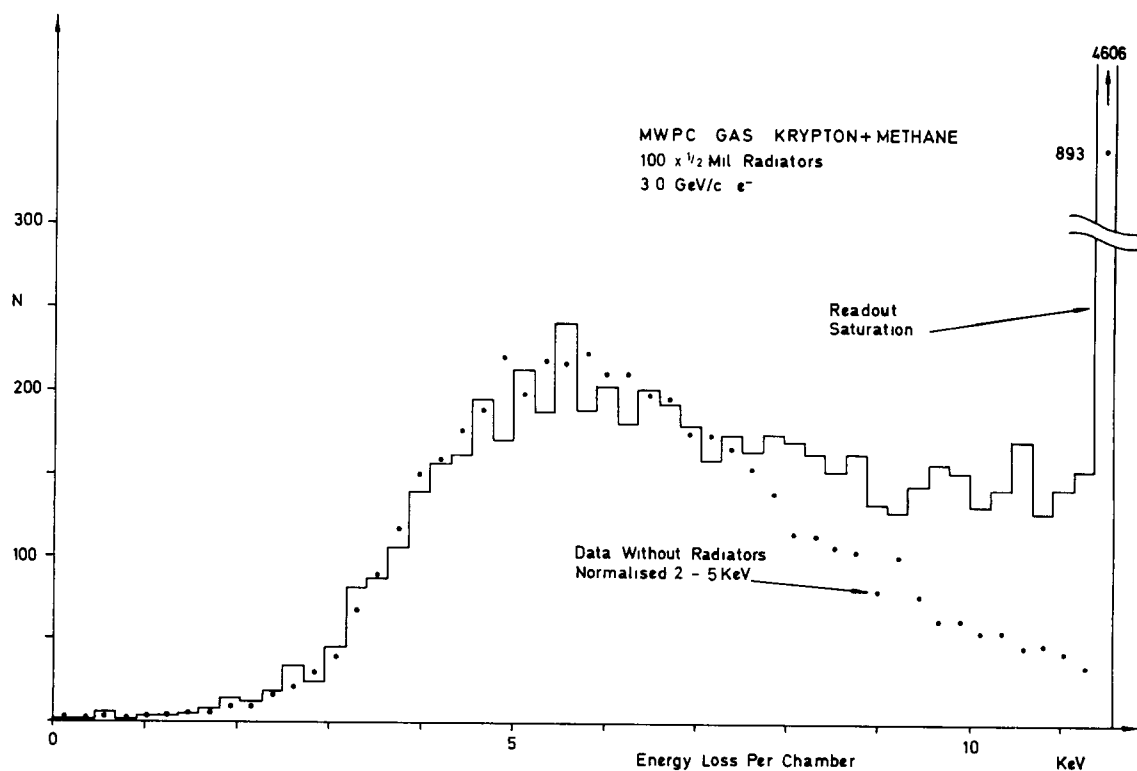


Fig 5b As for fig 5a but for chambers filled with 93% krypton + 7% methane. The dotted distribution has been normalised to equal the histogram area in the 2-5 keV region

be associated with a transition radiation photon — this part of the distribution is 'pure' ionization energy loss. So we can match the shapes of the no-radiator and with-radiator distributions below 4 keV, this has been done by normalising to the same number of events in the 1 → 3 keV interval. The result is the shape marked by dots superposed on the histogram of fig 5a, this then also shows the number of 'pure' ionization loss signals *above* 3 keV. In fact the ionization-loss shape follows the histogram well up to about 4.5 keV, confirming that there are very few photons of energy less than 3 keV entering the chambers.

As the average number of transition radiation photons detected in each chamber is less than one we can estimate a lower limit to the number of detected photons, N_γ , from the number of pulses in excess of the ionization-loss shape. The result is 3.6 ± 0.7 summed over all 11 chambers per incident electron; the error is mainly due to systematic effects, such as relative calibrations, but is *not* affected by the energy saturation in the readout system. Fig 5b shows the data for krypton filling with its greater efficiency for photon detection, in this case $N_\gamma = 5 \pm 0.5$.

The figures for N_γ and also total energy deposition for different radiator configurations and momenta are summarised in table 2. The effect of saturation is that the mean energies given in table 2 are systematically low. Using information from the channels with highest saturation and assuming a linear fall off above the saturation point, an estimate of the error has been made, this varies from 2–3% for the π -meson data to a shift in the mean of about 10% for the electron data in krypton with $\frac{1}{2}$ mil radiators.

Table 2 includes two sets of data, rows 1 and 6, for which no transition radiation effect should be observed. Row 1 is for 3 GeV/c mesons passing through the $\frac{1}{2}$ mil radiators and row 6 gives data for 3 GeV/c electrons passing through equivalent absorbers consisting of single sheets of plastic 50 mil thick. In neither case is a significant effect observed. The values of N_γ for 1 and 6 can be taken as indicating the uncertainty in the determination of this quantity, this perhaps suggests that the assigned errors, which are based on an estimated 5% uncertainty in relative calibration of runs made at different times, are conservative.

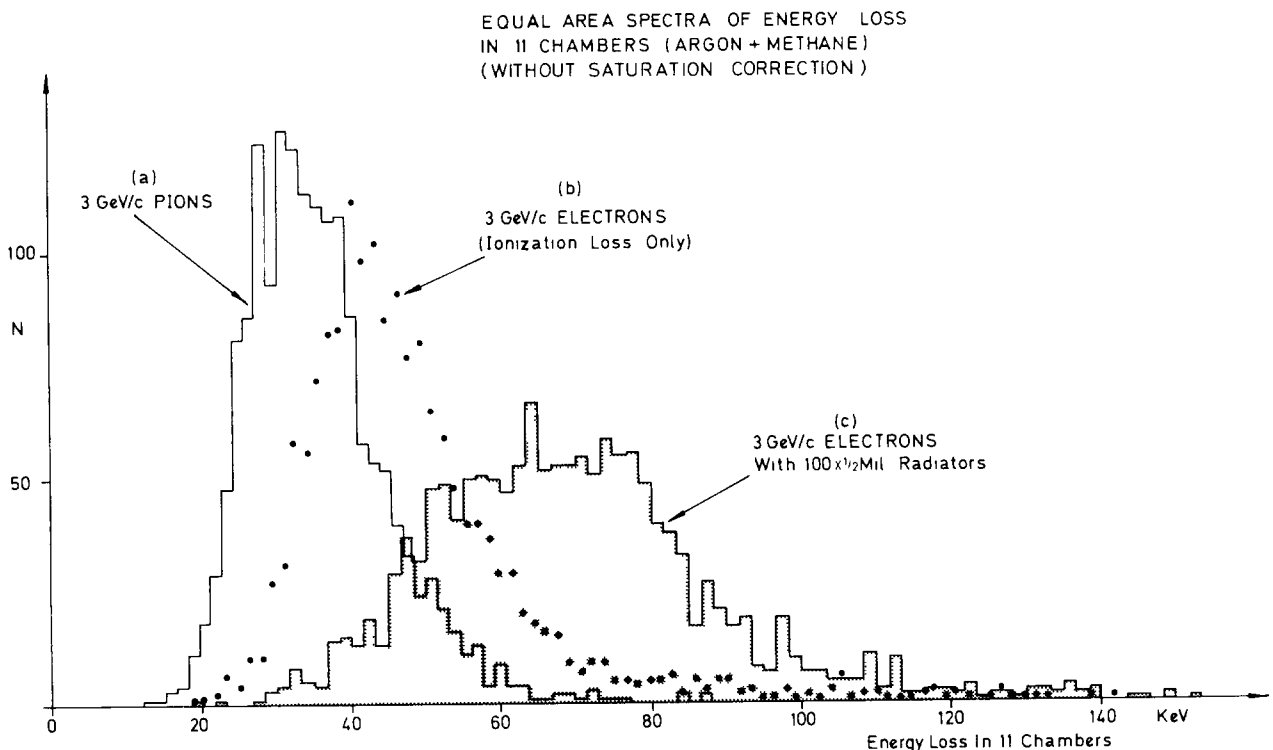


Fig 6 This shows the distributions of total energy deposited in 11 chambers plotted with equal areas for the three cases: 3 GeV/c τ^- mesons, 3 GeV/c electrons without radiators, and 3 GeV/c electrons with $\frac{1}{2}$ mil radiators, chamber gas 93% argon and 7% methane. Saturation in some of the readout channels causes a systematic underestimate of the number of large values.

The yield from $\frac{1}{8}$ mil foils is significantly lower than that for $\frac{1}{2}$ mil foils. This thickness dependence, already observed by Yuan et al.⁷⁾, is related to the coherence between the radiation from the leading and trailing interfaces of the foil and the observed drop in yield is in reasonable agreement with that expected when the thickness falls below the value of the formation zone.

The one run (row 8, table 2) made with slabs of 2" thick Styrofoam as radiators confirms earlier reports^{2,9)} that transition radiation is generated in this material, in this case the yield was about half that obtained with 100 $\frac{1}{2}$ mil mylar foils as radiator.

Row 7 in table 2 gives results obtained when the $\frac{1}{2}$ mil. foils were tilted at an angle of 30° to the incident 3 GeV/c electron beam. The result is close to that obtained for normal incidence (row 3).

Fig 6 shows three distributions of the sum of pulse heights from all eleven chambers filled with argon + methane. On the left, (a), is that for 3 GeV/c π^- -mesons, on the right and shaded, (c), is that for 3 GeV/c electrons passing through the $\frac{1}{2}$ mil radiators; the one in the middle, (b) is for 3 GeV/c electrons without radiators. The difference between π^- -mesons and electrons (no radiators) due to the relativistic rise is clear, as also is the upward shift of distribution (c) due to transition radiation.

Fig 7 shows the corresponding distributions for krypton + methane in the chambers. These are a further demonstration of the greater efficiency of krypton for the detection of photons, associated with the K absorption edge at 14.3 keV. The results show a significant relative displacement of the distributions for electrons with and without radiators and suggest that particle identification is possible by the detection of transition-radiation in the presence of ionization loss.

The authors are grateful to Dr J. G. Loken for writing the programme to measure the film on the Oxford PEPR. They also wish to thank the staff of the Bevatron and Lawrence Berkeley Laboratory for their aid and hospitality. Dr M. L. Stevenson is thanked for his assistance in the early stages of the experiment. Several discussions with members of the Brookhaven group working on transition radiation have been very useful.

The A. E. C. (Hawaii), N. S. F. (Maryland) and the R. H. E. L. (Oxford) are thanked for financial support.

References

- 1) V. L. Ginzburg and I. M. Frank, Soviet Phys. - JETP **16** (1946) 15.

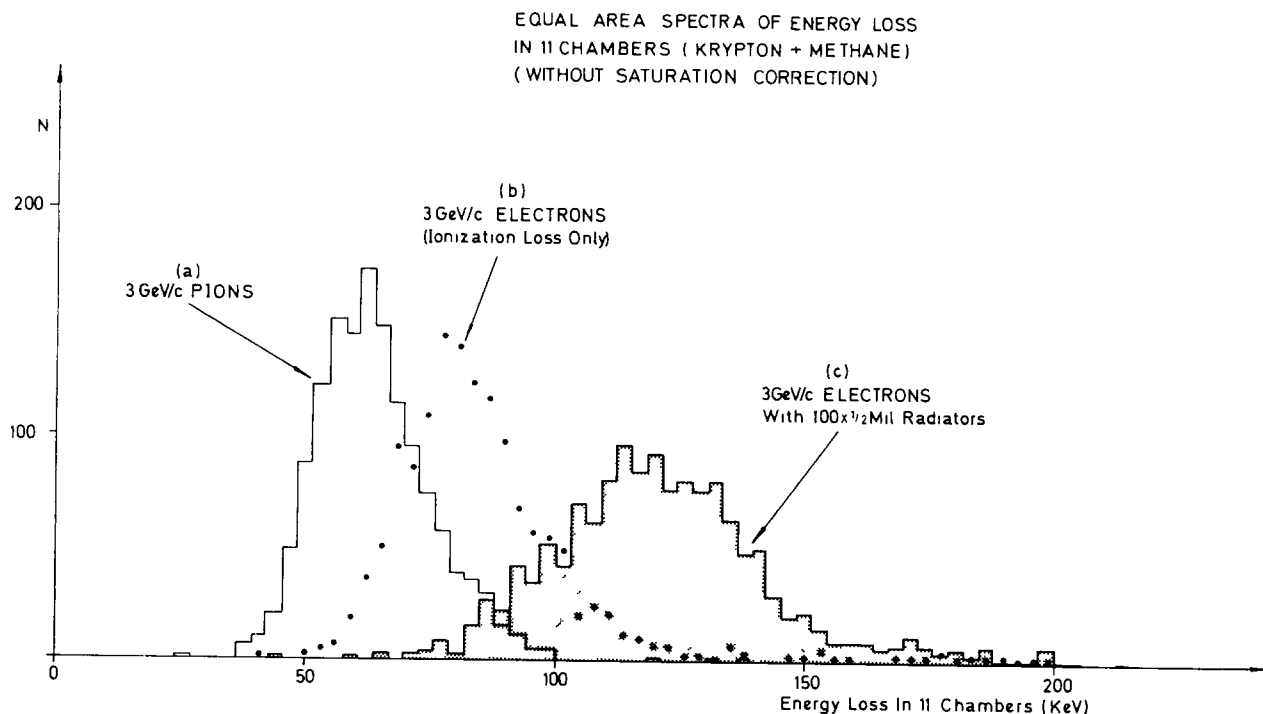


Fig 7 As for fig 6 but with a gas mixture of 93% krypton + 7% methane

- 2) A I Alikanian, K M Avakina, G M Garibian, M P Lorikian and K K Shikhiarov, *Phys Rev Letters* **25** (1970) 635
- 3) A I Alikhanian, K A Ispirian, A G Oganessian and A G Tamanian, *Nucl Instr and Meth* **89** (1970) 147
- 4) A A Franghian, F R Haratjunian, G A Hekimian, A A Nasarian and G B Torgomian, *Phys Letters* **34B** (1971) 227
- 5) G M Garibian, Yerevan Preprint E○N-T○-13 (1970) This article contains references to many other papers on transition radiation
- 6) L Yuan, C L Wang and S Prunster, *Phys Rev Letters* **23** (1969) 496
- 7) L Yuan, C L Wang, H Uto and S Prunster, *Phys Rev Letters* **25** (1970) 1513
- 8) L Yuan, C L Wang, H Uto and S Prunster, *Phys Letters* **31B** (1970) 603
- 9) H Uto, L Yuan, G Dell and C L Wang, *Nucl Instr and Meth* **97** (1971) 389
- 10) These results were presented in preliminary form at the Am Phys Soc Meeting (Washington, April 1972)
- 11) R W Ellsworth, J MacFall, P K MacKeown and G B Yodh, *Proc 6th Inter-Am Sem Cosmic radiation*, vol 2 (La Paz, Bolivia, 1970) p 344
- 12) t_f is a function of γ , the energy and angle of emission of the photon and the foil plasma frequency, for example the value of t_f for emission of 10 keV photons at an angle of $1/\gamma'$ (the peak of the angular distribution) by a particle of $\gamma = 6\,000$ entering mylar is $\sim \frac{1}{4}$ mil¹³⁾
- 13) 1 mil equals 10^{-3} in
- 14) S Parker, R Jones, J Kadyk, M L Stevenson, T Katsura, V Z Peterson and D Yount, *Nucl Instr and Meth* **97** (1971) 181
- 15) Although krypton is radioactive (since atmospheric testing of nuclear bombs introduced fission products) this is not a problem in this experiment since data is taken in coincidence with beam defining counters
- 16) J P Berge, C B Brooks, P G Davey, J F Harris and J G Loken, *Proc 2nd Intern Colloq PEPR* (MIT, Cambridge, Mass, May 1970) Also see C B Brooks, P G Davey, J F Harris, J G Loken and C A Wilkinson, *Conf Machine perception of patterns and pictures*, to be published by Institute of Physics
- 17) O Blunck and S Leisegang, *Z Physik* **128** (1950) 500
- 18) G Knop, A Minten and B Nellen, *Z Physik* **165** (1961) 533
- 19) Z Dimcovski, J Favier, G Charpak and G Amato, *Nucl Instr and Meth* **94** (1971) 151
- 20) P V Ramana Murthy, *Nucl Instr and Meth* **63** (1968) 77
- 21) The parameter b^2 , defined by Blunck and Leisegang¹⁷⁾, has the value 164 for 3 GeV/ $c\pi^-$ -mesons crossing a single chamber, and ~ 15 for a chamber of thickness eleven times this
- 22) D West, *Proc Roy Soc A* **66** (1953) 306
- 23) R Sternheimer and R F Peierls, *Phys Rev B* **3** (1971) 3681